Received Date:

Revised Date:

Accepted Date:

Article Type: Research Article

Prediction of skin dose in low-kV intraoperative radiotherapy using machine learning models trained on results of in vivo dosimetry

Michele Avanzo[1], PhD, Giovanni Pirrone[1], PhD, Mario Mileto[2], MD, Samuele Massarut[2], MD, Joseph Stancanello[1], PhD, Milad Baradaran-Ghahfarokhi[1], PhD, Alexandra Rink[3], PhD, Loredana Barresi[1], PhD, Lorenzo Vinante[4], MD, Erica Piccoli[2], MD, Marco Trovo[5], MD, Issam El Naqa[6], PhD, Giovanna Sartor[1], PhD

[1]Division of Medical Physics, [2]Department of Breast Surgery, and [4]Radiation Oncology, Centro di Riferimento Oncologico di Aviano (CRO) IRCCS, 33081 Aviano, PN, Italy

[3] Department of Radiation Physics, Princess Margaret Cancer Centre, ON M5G 2M9, Canada

[5] Department of Radiation Oncology, Udine General Hospital, 33100 Udine, UD, Italy.

[6] Department of Radiation Oncology, Physics Division, University of Michigan, Ann Arbor, MI 48103-493 (USA)

Keywords: in vivo, radiochromic, breast, cancer, intraoperative, IORT, machine learning

Corresponding Author

Michele Avanzo, PhD

Division of Medical Physics, IRCCS Centro di Riferimento Oncologico Aviano

Mail address: Via F.Gallini 2, 33081 Aviano, PN, Italy

Phone: +39 0434659175

e-mail: mavanzo@cro.it

Financial Support/Funding: The present research was in part supported by CRUP – Friuli Exchange Program (grant CUP J38C13001310007) and in part by 5x1000 (fund J32F16001310007)

Conflict of interest: The authors have no conflicts to disclose.

Running title: **Prediction of skin dose in kV-IORT**

Abstract

Purpose: To implement a machine learning model to predict skin dose from targeted intraoperative (TARGIT) treatment resulting in timely adoption of strategies to limit excessive skin dose.

Methods: A total of 283 patients affected by invasive breast carcinoma underwent TARGIT with a prescribed dose of 6 Gy at 1 cm, after lumpectomy. Radiochromic films were used to measure the dose to the skin for each patient. Univariate statistical analysis was performed to identify correlation of physical and patient variables with measured dose. After feature selection of predictors of *in vivo* skin dose, machine learning models stepwise linear regression (SLR), support vector regression (SVR), ensemble with bagging or boosting, and feed forward neural networks were trained on results of *in vivo* dosimetry to derive models to predict skin dose. Models were evaluated by 10-fold cross validation and ranked according to root mean square error (RMSE) and adjusted correlation coefficient of true versus predicted values (adj-R^2).

Results: The predictors correlated with in vivo dosimetry were the distance of skin from source, depth-dose in water at depth of the applicator in the breast, use of a replacement source, and irradiation time. The best performing model was SVR, which scored RMSE and adj-R^2, equal to 0.746 (95% confidence intervals, 95%CI 0.737,0.756) and 0.481 (95%CI 0.468,0.494) respectively, on the 10-fold cross-validation.

Conclusion: The model trained on results of in vivo dosimetry can be used to predict skin dose during setup of patient for TARGIT and this allows for timely adoption of strategies to prevent of excessive skin dose.

1. Introduction

An intraoperative radiotherapy (IORT) technique called TARGIT (targeted intra-operative radiotherapy) has been developed based on the Intrabeam system (Carl Zeiss, Oberkochen, Germany). In this technique a point-source, emitting low energy X-rays of 50 kVp coupled with a spherical applicator, is inserted into the surgical bed. The irradiation is administered soon after the primary tumor resection during the same operative session. The target tissue is the breast volume surrounding the excised tumor, wrapped around the radiotherapy source soon after the primary surgery. Two multi-

center prospective randomized trials, Targit-A and Targit-B, are currently testing the clinical efficacy of TARGIT, as partial breast technique in selected early-stage low-risk breast cancer patients, and as a boost to the tumor bed before conventional whole breast irradiation (WBRT) for high risk patients, respectively[1].

The skin represents the main organ at risk in TARGIT, because of its proximity to the source. A few cases of dermatitis and skin necrosis have been reported in early reports [2,3] as well as more recently [4] on this technique. No complications have been reported to other organs such as rib cage, lungs and heart, receiving a lower dose of radiation because of their larger distance from the radiation source and steep dose fall-off. Safety levels for skin effects as low as 1 Gy[5] or 2 Gy[6] have been recommended to the skin after single fraction low kV irradiation. A dose of 6 Gy has been identified as a reasonably threshold for transient skin injury. One case of grade 2 dermatitis was reported after IORT delivered as a boost prior to WBRT where dose measured by in vivo dosimetry was 8.42 Gy[7].

As skin dose can be critical for IORT, many studies focused on developing techniques to measure in vivo dose to the skin using different types of dosimeter, including radiochromic films[8], Thermo-Luminescent-Dosimeters (TLDs)[9,10], and optically stimulated luminescent dosimeters (OSLDs)[11]. In vivo measurements of dose are also essential as they help identifying systematic and random errors in treatment delivery[12,13]. Currently, individual pretreatment calculation of skin dose is challenged by the lack of treatment planning, mainly due to unsolved difficulties in installing useful in-room imaging systems, one of the major limitations of IORT techniques[14].

In the present study we want to implement a model to estimate dose to the skin in TARGIT before beginning of the IORT treatment. This tool would allow timely adoption of strategies to prevent excessive skin dose, such as placing a saline solution–soaked gauze as a spacer around the applicator, in order to increase source to skin distance. For this purpose, we use statistical and/or machine learning algorithms able to infer a hypothesis (the function/model), to predict the labels (skin dose) of out-of-sample observations[15,16,]. With the goal of achieving the best possible accuracy, the models are trained on data from in vivo skin dosimetry performed with an established technique on a large cohort of patients during more than four years of TARGIT practice at our centre.

2. Methods and materials

2.1 Patient data and follow-up

From October 2013 to March 2018, 283 patients with invasive breast carcinoma underwent TARGIT after lumpectomy. Patients and treatments relevant data are summarized in Table 1.

Patients were evaluated by expert breast surgeons during the three days after lumpectomy and then weekly until the complete wound healing. Incidences of acute toxicities, and in particular acute skin reactions, were collected during the first months after IORT. Subsequent clinical follow up was scheduled every six months during the first three years after IORT, and then yearly. Bilateral

mammography and ultrasonography were performed annually and late toxicities were evaluated during the follow up visits.

2.2 In vivo dosimetry

During surgery, a wide local excision was carried out to remove the tumor. A spherical applicator with the proper size was chosen based on the excision cavity. A purse-string suture was then applied deeply to the whole cavity edges[17]. The treatment delivery time was calculated by the Medical Physics staff using the Intrabeam Treatment Software, in order to deliver a prescribed dose of 5 or 6 Gy to 1 cm from the applicator surface in water, with 50 kVp, 40 µA X-rays. The source was attached to the applicator and the gantry. Once the applicator was in place, the purse-string was tightened carefully so that the breast tissue wrapped around the applicator. In order to prevent excessive irradiation of the skin, the edges were kept at least 1 cm away from the applicator shaft[3].

Gafchromic EBT3 (Ashland Special Ingredients, Bridgewater, NJ, USA) films were used to measure dose to the skin on patients who underwent TARGIT. Because the sensitive layer of the film is 0.125 mm from the surface of the patient, correction for the effective point of measurement is negligible for radiochromic films[18], and it can be safely assumed that EBT3 measures directly the skin dose. Before the surgical procedure, pieces of radiochromic films were wrapped by a nurse of the surgical staff in a thin sterile envelope. Films were calibrated in air using the Intrabeam with spherical applicators, following a previously established procedure[8].

Two sheets of tungsten-impregnated rubber (0.1 mm lead equivalent; Carl Zeiss Surgical) were placed over the wound, thus covering also the films, to reduce the amount of stray radiation in the operating room during irradiation. Once the treatment finished, the purse-string was cut, and the applicator and the shield were removed[17]. Films were collected and scanned using an Epson Expression 1680 (Epson-Seiko Corporation, Japan) flatbed scanner, and film images were converted into dose matrices according to a multi-channel scanning protocol[19-21]. For measurement of dose and its uncertainty, average dose and standard deviation were calculated inside a region of interest (ROI) consisting of a 2x2 mm^2 square around the highest dose reading on the piece of film and positioned at least 2 mm from the film edges.

2.3 Statistical analysis

For each patient, age, laterality of breast cancer, and quadrant of breast (inner/midline/outer and upper/medial/lower) where the source was introduced were registered. Before placing the dosimeter, the point where the spherical applicator is at minimum depth under the patient skin was found by palpation. Then the minimum depth, d_{min} of the spherical applicator was measured by insertion of a needle and measurement of the extent of needle insertion. The film was placed at the same position on the skin from which d_{min} was measured (Supplementary material Figs. 1a-d). The distance from the point of measurement to the point of insertion of the source along the skin was also collected using a

ruler. The value of depth-dose curve at d_{min}, $D(d_{min})$ calculated by the Intrabeam software was also recorded, as it was previously postulated to be related to measured skin dose[10,22].

The prescribed dose, diameter of the spherical applicator, and irradiation time were recorded among the variables related to treatment. Our Intrabeam system has two x-rays sources (serial numbers 321 and the 338, respectively). When one of the two sources was not available because of maintenance, repair or recalibrations, Zeiss provided a temporary replacement. It was also then recorded if source 1, 2 or a replacement source was used. Univariate statistical analysis was performed to find correlation of variables with measured dose, using the Spearman rank correlation test for ordinal variables, while the Kruskal-Wallis rank test was used for categorical variables.

2.4 Model implementation

Before training models, outliers were removed by performing a nonlinear multivariate regression using support vector machine (SVM), which was preferred because of its capability to deal with linear and non-linear functional mappings. The data points whose residuals were three times higher than the standard deviation (larger than 99% confidence level) of the residuals of the entire dataset, were considered as possibly caused by incorrect measure of distance and/or depth, and were removed from analysis as outliers. Then, the least absolute shrinkage and selection operator (LASSO) [23] was applied in order to eliminate redundant variables that are likely not to be related to the measured dose.

First, an univariable linear regression was attempted using the most relevant predictor, $D(d_{min})$ with the aim to investigate if in vivo dosimetry can be predicted also using a uni-metric model. Then, the following statistical and machine learning algorithms were trained on the dataset (predictors and in vivo dose from patients) to build multi-metric models able to predict in vivo dose:

1) **Stepwise linear regression (SLR),** which results in a linear multi-metric model; terms from a linear or generalized linear model are removed or added in order to find the subset of variables in the data set resulting in the smallest model with lowest prediction error [24].

2) SVR is the regression version of SVM, a supervised machine learning technique which, by means of a kernel function, projects the data into a higher-dimensional feature space and can perform linear regression in this high-dimension feature space. SVR tolerates errors that are inferior to a margin, thus providing a tradeoff between goodness of fit and model robustness [25].

3) Ensemble machine learning (EML) uses multiple learners aggregated into a single learner. We used for weak learners Decision Trees, a popular concept in machine learning [15]. In EML **with bagging (EML/bag)**, a group of decision trees is trained, and the algorithm randomizes training samples by resampling with replacements; second, at each branching step it chooses an attribute to split among a randomly selected subset of attributes. After a bag of trees is trained, prediction is made for all the individual trees and the most frequent class selected by the trees is taken as a final result [26].

4) EML with boosting (EML/boost), where decision trees are trained sequentially on subsets containing the data that were misclassified in previous training steps, then they are feedback in order to boost performance[27].

5) Feed-forward neural network (NN) using Bayesian regularization training algorithm. Neural networks are described as parallel-distributed computational models that consist of many nonlinear elements arranged in patterns that imitate biological nervous systems [28].

In order to compare the performance of the different models, we used the root mean square error (RMSE) which describes the difference among modeled and measured dose, and the adjusted correlation coefficient (adj-R^2) of predicted and measured data, which reflects the goodness of fit of the model to the population taking into account the sample size and the number of predictors used [29].

2.5 Cross validation and analysis of sample size

In order to test out-of-sample accuracy, 10-fold cross-validation, where the 267 patients were randomly partitioned into 10 subsamples of nearly equal size, was performed. 9 subsamples were used to train the model, which was validated on the 10^{th} subsample. Then the training and validation subsamples were rotated, so that all patients are used once in the validation subsample. RMSE and adj-R^2 were calculated from results in the validation subsamples ($RMSE_v$ and adj-R^2_v). The whole process was repeated 100 times in order to derive average values and 95% confidence intervals (95% CI) of $RMSE_v$ and adj-R^2_v.

In order to determine if the dataset was large enough to build a multivariable model, the SVR was performed on randomly chosen samples of increasing number of patients. The procedure was repeated 1000 times for each sample size. The p-value of a t-test (zero vs nonzero coefficient in the SVR) was performed for the three most predictive variables: $D(d_{min})$, distance and use of a replacement source. The sample size was considered large enough to build a multivariable model when all these three variables reached a p-value under the 0.05 significance level.

3. RESULTS

3.1 Patients results

The mean measured skin dose was 3.21 Gy, (95% CI 1.53-5.38 Gy). No acute radiation injury to the skin, necrosis, skin breakdown or delayed wound healing was observed during the patients' follow-up. None of the patients showed evidence of significant clinical complications. No late toxicity (i.e. hyperpigmentation, telangiectasia, ulceration) was found. In patients that received WBRT after TARGIT, no additional risk of skin toxicity was detected in the skin area close to the lumpectomy.

3.2 Statistical analysis

The results of the univariate statistical analysis are shown in Table 2. The in vivo measured dose was strongly ($p<0.0001$) correlated with $D(d_{min})$, distance of film from the applicator, and applicator diameter. Significant but weaker correlations ($p<0.05$) were found with prescribed dose, irradiation time and Intrabeam source used. In vivo dose was uncorrelated with tumor laterality, point of insertion of the source, and patient age.

3.3 Models development

A total of 16 measurements (5.6%) were removed from the analysis as outliers. In the feature selection, the following variables were selected, and then passed to the machine learning algorithms: prescribed dose, $D(d_{min})$, use of a replacement source, applicator diameter, laterality of breast (left and right), outer and superior position of the source, distance of the film, and d_{min}.

The plots of estimated versus measured dose from calibration and validation of machine learning methods are shown in Fig. 1. The performances in training and 10-fold cross-validation are compared in Table 3, and the distributions of $RMSE_v$ and adj-R^2_v from the 10-fold cross-validation are shown in Fig 2.

The univariable linear regression of in vivo dose versus $D(d_{min})$ had a lower $RMSE_v$ and Adj-R^2_t (Wilcoxon Ranksum test $p<<0.05$) than multi-metric machine learning models in the cross-validation, and was excluded in the remainder of the analysis. The machine learning model with the best scores in the 10-fold cross validation, lowest $RMSE_v$ and highest adj-R^2_v, was the SVR. The $RMSE_v$ and adj-R^2_v were significantly different among all models (Wilcoxon Ranksum test, $p<<0.05$). Therefore, SVR was considered as our best performing model ($RMSE_v = 0.746$, adj-$R^2_{v=}$ 0.481), followed by SLR. The learning curve power analysis (Fig. 3) shows that the p-values for inclusion of the three most predictive variables in the SVR model were all below 0.05 for sample size larger than 91 patients. Therefore the dataset of 267 patients used in the analysis was considered largely adequate to build multivariable models predictive of in vivo dose.

4. Discussion

Studies reported results of in vivo dosimetry in patients who received TARGIT as soon as the skin was recognized as the main organ at risk during this procedure. In vivo dosimetry in a series of 72 patients resulted in average measured dose of 2.9 Gy, with 11% of readings ≥ 6 Gy[10]. Measurements with TLD on the skin at distances of 5 and 15 mm from the incision on 57 patients resulted in maximum dose of 2.93 Gy on average[9]. The distribution of skin doses measured in our patient dataset are in agreement with the previous studies.

It is no surprise that, in our results, the variable with the strongest correlation was $D(d_{min})$ in water, as it describes the dependency of dose from the applicator diameter, depth of the applicator, the prescribed dose, and the amount of tissue between the skin and the applicator. However, the linear regression

model based on $D(d_{min})$ resulted in poor predictive capability compared to other models, thus showing the advantage of using multi-metric machine learning to predict skin dose.

The univariate statistical analysis confirmed the dependencies of in vivo measured skin dose on distance from the measured point from the applicator shaft, in agreement with previous reports[9,10]. The distance from the applicator shaft was an independent predictor of skin dose possibly because, for a fixed depth, an increase of distance implies a different geometry of irradiation, where the applicator is more oblique.

Monte Carlo simulation of a breast phantom with realistic tissue compositions and skin layers, demonstrated that in vivo dose depends on the size of applicator[22], as well as the amount of breast tissue between the applicator and the skin. In the study of Fogg et al[9], the ratios between average doses measured with TLDs at 5 mm and at 15 mm from the point of insertion were 1.47, 1.22, 1.24 and 1.11 for the 3.5, 4.0, 4.5 and 5.0 cm applicators respectively. This effect has been explained with more penetrating beam spectrum with larger applicators[22], but it should be also noted that the use of larger applicators is preferred on patients with larger breast size, as confirmed by correlation in our dataset among d_{min} and applicator diameter (Spearman correlation test $p<<0.0001$).As expected, in the univariate analysis measured dose was also correlated with other variables related to the quantity of radiation emitted, such as the irradiation time and the prescribed dose which is specified, according to the TARGIT protocol, as the dose at 1 cm from the applicator surface in water. Seven units were used for spare sources, when one of the two sources were not available because of maintenance, repair or recalibrations, and the use of a replacement source was related to in vivo dose. Dosimetric and spectrum characteristics different from the other sources may explain this result. Differences in the output dose rate of different sources has been reported [30], however, given that the dose rate is checked and, if necessary, readjusted before each treatment[4], are unlikely to affect measured dose. Small differences in the various structures involved in the generation of x-rays, including the electron source, the beam deflector as well as the gold target, such as between manufactured and ideal target thickness, could change photon spectra and doses between different sources, thus explaining a change of dose[22]. In our results, the feature selection successfully removed those variables that are not correlated with measured dose (e.g. age) and those that suffer from collinearity and are redundant, such as d_{min}, which is related to $D(d_{min})$.

Among the multi-metric machine learning models, SVR showed the best performance (lowest RMSE and highest adj-R^2) on the cross-validation and therefore we consider it as the model of choice. This result is in agreement with other reports where SVM classifiers were among the best performing machine learning methods[31]. The second best method, SLR, has the advantage to provide a simple calculation to be used in an operating room. For this reason, the formula resulting from the SLR is shown in table 4.

Our machine learning models were trained on a dataset of 283 patients, which is the largest published results of in vivo dosimetry in IORT. The plot of the model residuals shows that the in vivo dose calculated by considered models have uncertainties. A possible explanation for the residuals could be the manual measurements of d_{min} and distance, whose accuracy could be improved, for example, by using ultrasound imaging to measure the thickness of breast tissue between the applicator and the point of interest. Skin dose may also vary because of variation of the compositions of the treated breast. Treatments are usually performed covering the patient surface over the applicator with a lead-rubber protection sheet whose backscatter could increase skin dose, however to a relatively small amount [14]. As all our treatments were performed with the protection sheet, it was not possible to verify how much the skin dose is dependent on its use.

By using the model recommended by this study, it is possible to anticipate measured in vivo dose from TARGIT in the operating room. This work shows that the machine learning approach can be applied to in vivo dosimetry, as successfully done in other areas of radiotherapy workflow, including error detection and prevention [16], treatment dose planning [32] and verification [33,34]. It also suggests that the results of in vivo dosimetry should be included among other categories of patient data in the electronic patient records in order to be available for automated data extraction with the aim of generating or improving prediction models for patient dose.

A word of caution is needed. The availability of the models provided here to predict skin dose should not prevent measured in vivo dosimetry to the skin, which remains fundamental as an independent quality check of radiotherapy identifying errors in delivery, e.g., caused by wrong calibration of the machine. In vivo dosimetry still holds as an effective method to validate the introduction and any modification to the delivery of this intraoperative technique by measuring dose to the skin and other critical structures as required.

5. Conclusion

This work shows the potential of extending the machine learning approach to in vivo dosimetry in IORT. Models for the prediction of in vivo dose to the skin in TARGIT were derived from measurements of skin dose performed for over four years at our center with a consistent technique. Of the machine learning models used, SVR was the best performing model, and can be used to predict and evaluate dose to the skin before treatment delivery and to adopt measures to minimize excessive dose to the skin.

TABLES AND FIGURES CAPTIONS

Table 1. Overview of patient and in vivo dosimetry data. For dichotomic variables, the number (percentage) of patients, and for continuous variables, the average value with 95% confidence intervals are specified.

Table 2. Results of univariate statistical analysis of variables related to treatment and in vivo dosimetry. For ordinal variables, the p-value and correlation coefficient, r, from the Spearman rank correlation test are reported, while for categorical variables the Kruskal-Wallis rank test's p-value is shown

Table 3. Assessment of machine learning models with different methods. $RMSE_t$, $Adj\text{-}R^2_t$, $RMSE_v$, $Adj\text{-}R^2_v$, are root mean square error, and adjusted R^2 in the training and validation datasets with 95% confidence intervals.

Table 4. Estimated coefficients from the SLR modelling with standard error (SE) and p-value for inclusion in the model.

Figure 1. Calibration and cross-validation of machine learning models.

Figure 2. Distribution of values of RMSE and adj-R^2 from 10-fold cross-validation repeated 100 times for multivariable machine learning models.

Figure 3. Analysis of statistical power of the study by learning curve. The p-value of t-tests (zero vs nonzero coefficient) for inclusion of the three most predictive variables of in vivo dosimetry in the SVR model is plotted against the number of patients used for training.

REFERENCES

1 J.S. Vaidya, M. Baum, J.S. Tobias, F. Wenz, S. Massarut, M. Keshtgar, B. Hilaris, C. Saunders, N.R. Williams, C. Brew-Graves, T. Corica, M. Roncadin, U. Kraus-Tiefenbacher, M. Sutterlin, M. Bulsara, D. Joseph, "Long-term results of targeted intraoperative radiotherapy (Targit) boost during breast-conserving surgery," Int. J. Radiat. Oncol. Biol. Phys. **81**, 1091-1097 (2011).

2 D.J. Joseph, S. Bydder, L.R. Jackson, T. Corica, D.J. Hastrich, D.J. Oliver, D.E. Minchin, A. Haworth, C.M. Saunders, "Prospective trial of intraoperative radiation treatment for breast cancer," ANZ J. Surg. **74**, 1043-1048 (2004).

3 B.H. Chua, M.A. Henderson, A.D. Milner, "Intraoperative radiotherapy in women with early breast cancer treated by breast-conserving therapy " ANZ J. Surg., **81**, 65-69 (2010).

4 Z. Maoz, S. Ayelet, L. Michelle, B. Arie, S. Eitan, Y.R. Ben, S. Mariana, "Short-term complications of intra-operative radiotherapy for early breast cancer," J. Surg. Oncol. **113**, 370-373 (2016).

5 T.B. Shope, "Radiation-induced skin injuries from fluoroscopy," Radiographics **16**, 1195-1199 (1996).

6 J. Geleijns and J. Wondergem, "X-ray imaging and the skin: radiation biology, patient dosimetry and observed effects," Radiat. Prot. Dosimetry **114**, 121-125 (2005).

7 J.J.B. Lee, J. Choi, S.G. Ahn, J. Jeong, I.J. Lee, K. Park, K. Kim, J.W. Kim, "In vivo dosimetry and acute toxicity in breast cancer patients undergoing intraoperative radiotherapy as boost," Radiat. Oncol. J. **35**, 121-128 (2017).

8 M. Avanzo, A. Rink, A. Dassie, S. Massarut, M. Roncadin, E. Borsatti, E. Capra, "In vivo dosimetry with radiochromic films in low-voltage intraoperative radiotherapy of the breast," Med. Phys. **39**, 2359-2368 (2012).

9 P. Fogg, K.R. Das, T. Kron, C. Fox, B. Chua, J. Hagekyriakou, "Thermoluminescence dosimetry for skin dose assessment during intraoperative radiotherapy for early breast cancer," Australas. Phys. Eng. Sci. Med. **33**, 211-214 (2010).

10 D.J. Eaton, B. Best, C. Brew-Graves, S. Duck, T. Ghaus, R. Gonzalez, K. Pigott, C. Reynolds, N.R. Williams, M.R.S. Keshtgar, "In Vivo Dosimetry for Single-Fraction Targeted Intraoperative Radiotherapy (TARGIT) for Breast Cancer," International Journal of Radiation Oncology*Biology*Physics **82**, e819-e824 (2012).

11 C. Price, A. Pederson, C. Frazier, J. Duttenhaver, "In vivo dosimetry with optically stimulated dosimeters and RTQA2 radiochromic film for intraoperative radiotherapy of the breast," Med. Phys. **40**, 091716 (2013).

12 P.D. Higgins, P. Alaei, B.J. Gerbi, K.E. Dusenbery, "In vivo diode dosimetry for routine quality assurance in IMRT," Med. Phys. **30**, 3118-3123 (2003).

13 M. Essers and B.J. Mijnheer, "In vivo dosimetry during external photon beam radiotherapy," Int. J. Radiat. Oncol. Biol. Phys. **43**, 245-259 (1999).

14 F.W. Hensley, "Present state and issues in IORT Physics," Radiat. Oncol. **12**, 37-016-0754-z (2017).

15 M. Avanzo, J. Stancanello, I. El Naqa, "Beyond imaging: The promise of radiomics," Phys. Med. **38**, 122-139 (2017).

16 M. Feng, G. Valdes, N. Dixit, T.D. Solberg, "Machine Learning in Radiation Oncology: Opportunities, Requirements, and Needs," Frontiers in Oncology **8**, 110 (2018).

17 J.S. Vaidya, M. Baum, J.S. Tobias, S. Morgan, D. D'Souza, "The novel technique of delivering targeted intraoperative radiotherapy (Targit) for early breast cancer," Eur. J. Surg. Oncol. **28**, 447-454 (2002).

18 T.A. Reynolds and P. Higgins, "Surface dose measurements with commonly used detectors: a consistent thickness correction method," J. Appl. Clin. Med. Phys. **16**, 358-366 (2015).

19 S. Devic, N. Tomic, C.G. Soares, E.B. Podgorsak, "Optimizing the dynamic range extension of a radiochromic film dosimetry system," Med. Phys. **36**, 429-437 (2009).

20 A. Micke, D.F. Lewis, X. Yu, "Multichannel film dosimetry with nonuniformity correction," Med. Phys. **38**, 2523-2534 (2011).

21 D. Lewis, A. Micke, X. Yu, M.F. Chan, "An efficient protocol for radiochromic film dosimetry combining calibration and measurement in a single scan," Med. Phys. **39**, 6339-6350 (2012).

22 F. Moradi, N.M. Ung, M.U. Khandaker, G.A. Mahdiraji, M. Saad, R. Abdul Malik, A.Z. Bustam, Z. Zaili, D.A. Bradley, "Monte Carlo skin dose simulation in intraoperative radiotherapy of breast cancer using spherical applicators," Phys. Med. Biol. **62**, 6550-6566 (2017).

23 T.P. Coroller, P. Grossmann, Y. Hou, E. Rios Velazquez, R.T. Leijenaar, G. Hermann, P. Lambin, B. Haibe-Kains, R.H. Mak, H.J. Aerts, "CT-based radiomic signature predicts distant metastasis in lung adenocarcinoma," Radiother. Oncol. **114**, 345-350 (2015).

24 F.G. R., "Stepwise Regression," in *Wiley International Encyclopedia of Marketing*, edited by Anonymous (American Cancer Society, 2010).

25 S. Chen, S. Zhou, F.F. Yin, L.B. Marks, S.K. Das, "Investigation of the support vector machine algorithm to predict lung radiation-induced pneumonitis," Med. Phys. **34**, 3808-3814 (2007).

26 D. Yang, G. Rao, J. Martinez, A. Veeraraghavan, A. Rao, "Evaluation of tumor-derived MRI-texture features for discrimination of molecular subtypes and prediction of 12-month survival status in glioblastoma " Med. Phys. **42**, 6725-6735 (2015).

27 R. Polikar, "Ensemble based systems in decision making," IEEE Circuits and Systems Magazine **6**, 21-45 (2006).

28 S. Lee and I. El Naqa, "Machine Learning Methodology," in *Machine Learning in Radiation Oncology: Theory and Applications*, edited by I. El Naqa, R. Li, M.J. Murphy (Springer International Publishing, Cham, 2015), pp. 21-39.

29 D.C. Montgomery and G.C. Runger, *Applied Statistics and Probability for Engineers*, Seventh ed. (Wiley, Hoboken, NJ, 2018).

30 K.S. Armoogum, J.M. Parry, S.K. Souliman, D.G. Sutton, C.D. Mackay, "Functional intercomparison of intraoperative radiotherapy equipment - Photon Radiosurgery System," Radiat. Oncol. **2**, 11 (2007).

31 M. Fernàndez-Delgado, E. Cernadas, S. Barro, D. Amorim, "Do we Need Hundreds of Classifiers to Solve Real World Classification Problems?" Journal of Machine Learning Research **15**, 3133-3181 (2014).

32 X. Zhu, Y. Ge, T. Li, D. Thongphiew, F.F. Yin, Q.J. Wu, "A planning quality evaluation tool for prostate adaptive IMRT based on machine learning," Med. Phys. **38**, 719-726 (2011).

33 G. Valdes, T.D. Solberg, M. Heskel, L. Ungar, C.B. Simone, "Using machine learning to predict radiation pneumonitis in patients with stage I non-small cell lung cancer treated with stereotactic body radiation therapy," Phys. Med. Biol. **61**, 6105-6120 (2016).

34 G. Valdes, M.F. Chan MF, S.B. Lim SB, R. Scheuermann R, J.O. Deasy, T.D. Solberg, "IMRT QA using machine learning: A multi-institutional validation", J Appl Clin Med Phys. **18**, 279-284 (2017)

Table 1.

Characteristics (N=283)	Data
Tumor site (inner/central/outer):	
- Inner:	54 (19.1%)
- Central	53 (18.7%)
- Outer	176 (62.2%)
Tumor site (inferior/central/superior)	
- Inferior	43 (15.2%)
- Central	77 (27.2%)
- Superior	163 (57.6%)
Prescribed dose	
- 6 Gy	262 (92.6%)
- 5 Gy	21 (7.4%)
Intrabeam source used, serial number	
- Source 1, #338	111 (39.2%)
- Source 2, #321	127 (44.9%)
- Temporary replacement	45 (15.9 %)
Applicator diameter (3.5 / 4 / 4.5 / 5 cm)	
- 3.5 cm	6 (2.1%)
- 4.0 cm	40 (14.1%)
- 4.5 cm	69 (24.4%)
- 5.0 cm	168 (59.4%)
Age [mean (95% CI)]	65 (34-85)
Depth of applicator [mean (95% CI)] (cm)	1.4(0.8-2.5)
Distance film-applicator [mean (95% CI)] (cm)	3.1(1.5-4.5)
Measured dose [mean (95% CI)] (Gy)	3.21(1.53-5.38)
Relative standard deviation of measured dose [mean (95% CI)] (%)	5.2 (2.1-9.9)

Table 1. Overview of patient and in vivo dosimetry data. For dichotomic variables, the number (percentage) of patients, and for continuous variables, the average value with 95% confidence intervals are specified.

Table 2.

Variable	p-value	r
Prescribed Dose (5 Gy or 6 Gy)	<0.05	0.1394
Irradiation time	<0.05	-0.1934
Distance of film from the applicator shaft	<0.0001	-0.2936
Depth of the applicator surface beneath the film (d_{min})	<0.0001	-0.5679
Calculated dose in water at $d_{min,}$ $D(d_{min})$	<0.0001	0.5751
Spherical applicator diameter	<0.0001	-0.2564
Age of the patient (y)	0.48	-0.0424
Intrabeam source 1,	0.387	
" source 2	0.2667	
replacement source	<0.05	
Breast laterality	0.27	
Inner/medial/outer insertion of source	0.14	
Superior/midline/inferior insertion of source	0.97	

Table 2. Results of univariate statistical analysis of variables related to treatment and in vivo dosimetry. For ordinal variables, the p-value and correlation coefficient, r, from the Spearman rank correlation test are reported, while for categorical variables the Kruskal-Wallis rank test's p-value is shown

Table 3.

Learning method	$RMSE_t$	Adj-R^2_t	$RMSE_V$(95%CI)	Adj-R^2_V(95%CI)
SLR	0.725	0.51	0.751(0.74,0.762	0.474(0.459,0.489)
SVR	0.714	0.525	0.746(0.737,0.756)	0.481(0.468,0.494)
EML Boost	0.536	0.732	0.767(0.747,0.79)	0.451(0.417,0.479)
EML Bag	0.611	0.652	0.760(0.749,0.770)	0.461(0.447,0.476)
NN	0.683	0.564	0.765(0.742,0.795)	0.453(0.41,0.487)

Linear regression on $D(d_{min})$	0.788	0.440	0.791(0.788,0.797)	0.439(0.408,0.467)

Table 3. Assessment of machine learning models with different methods. $RMSE_t$, Adj-R^2_t, $RMSE_v$, Adj-R^2_v, are root mean square error, and adjusted R^2 in the training and validation datasets with 95% confidence intervals.

Table 4.

Coefficient of SLR model	Estimate	Standard Error (SE)	p-value
(Intercept)	1,986	0,209	$1.2 \cdot 10^{-18}$
Distance	-0,246	0,048	$4.8 \cdot 10^{-7}$
$D(d_{min})$	0,408	0,027	$6.46 \cdot 10^{-37}$
Use of a replacement source	-0,555	0,124	$1.16 \cdot 10^{-5}$

Table 4. Estimated coefficients from the SLR modelling with standard error (SE) and p-value for inclusion in the model.

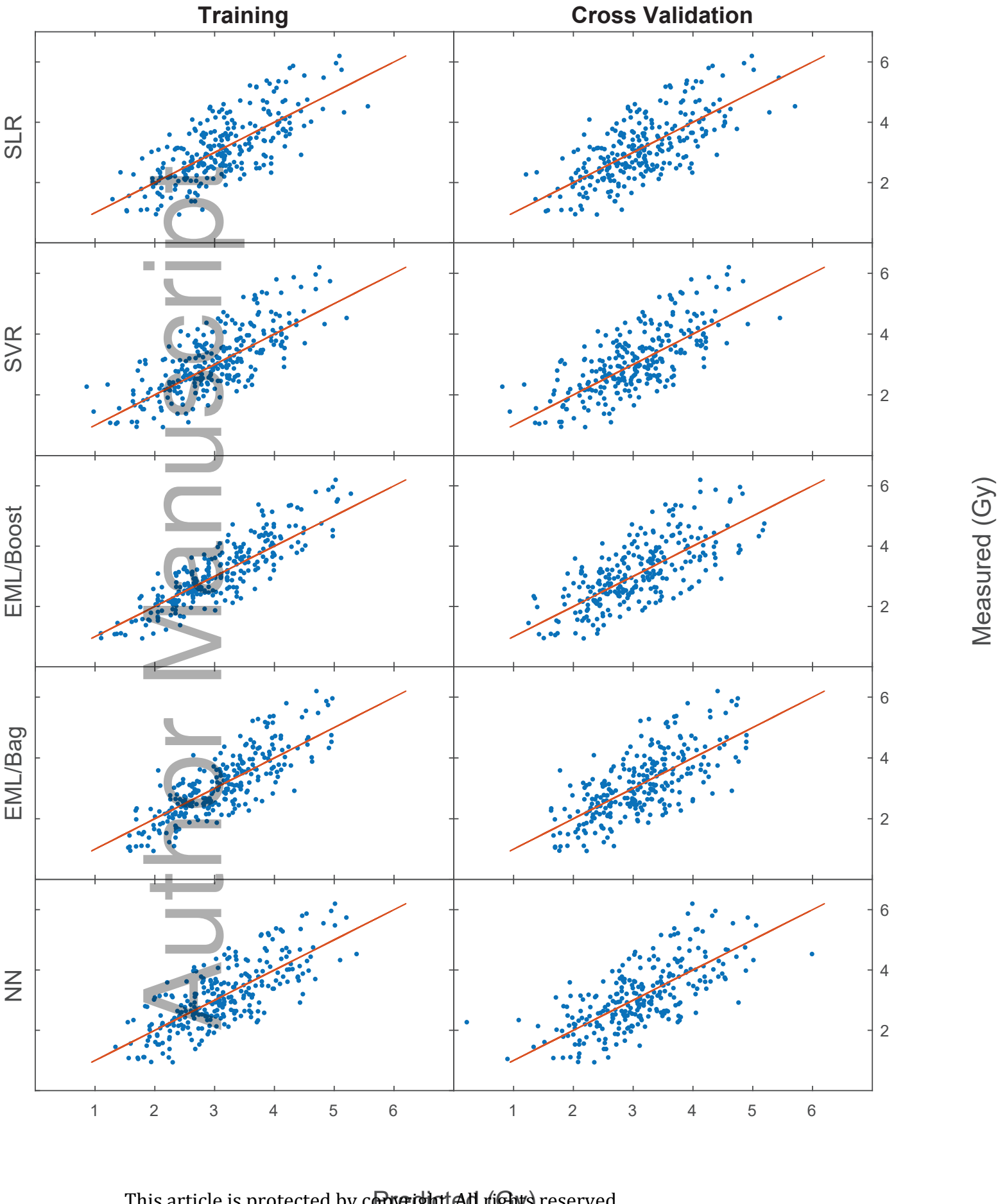

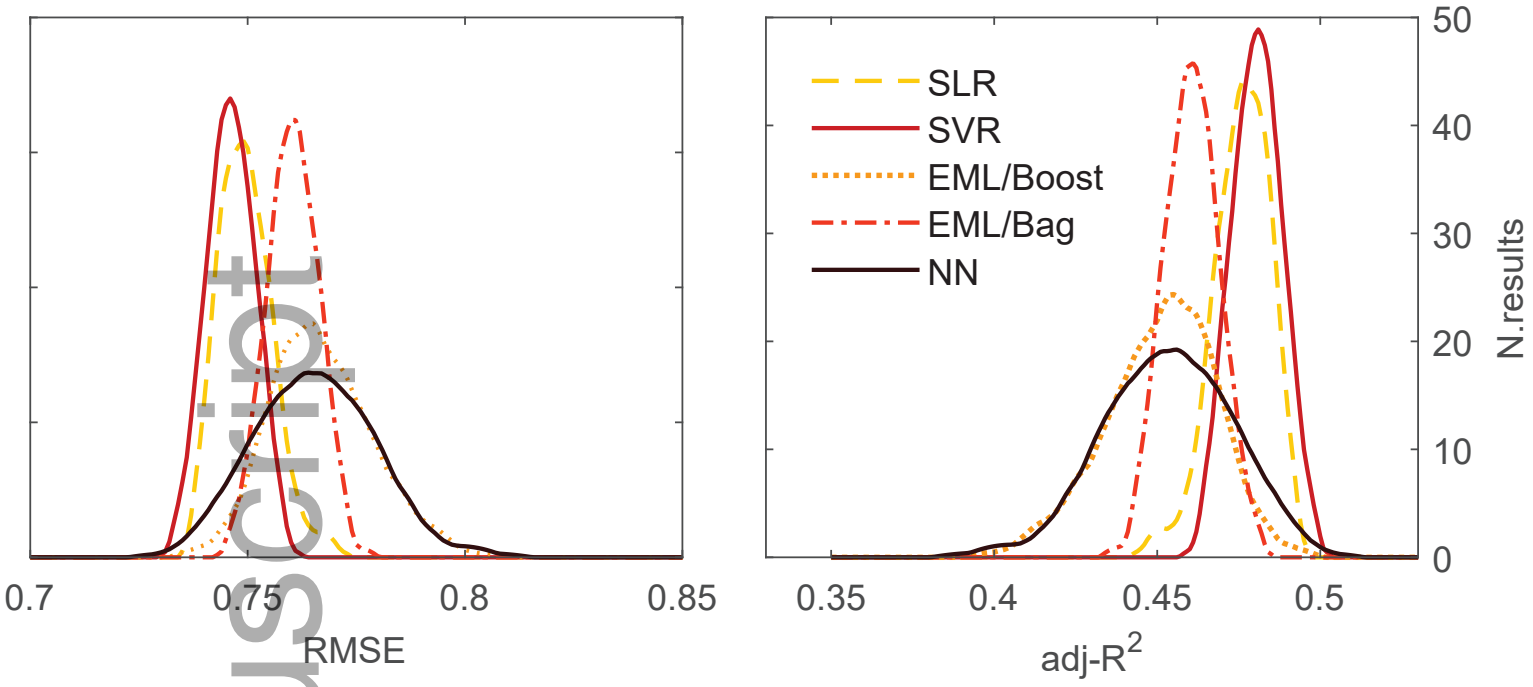

mp_13379_f2.eps

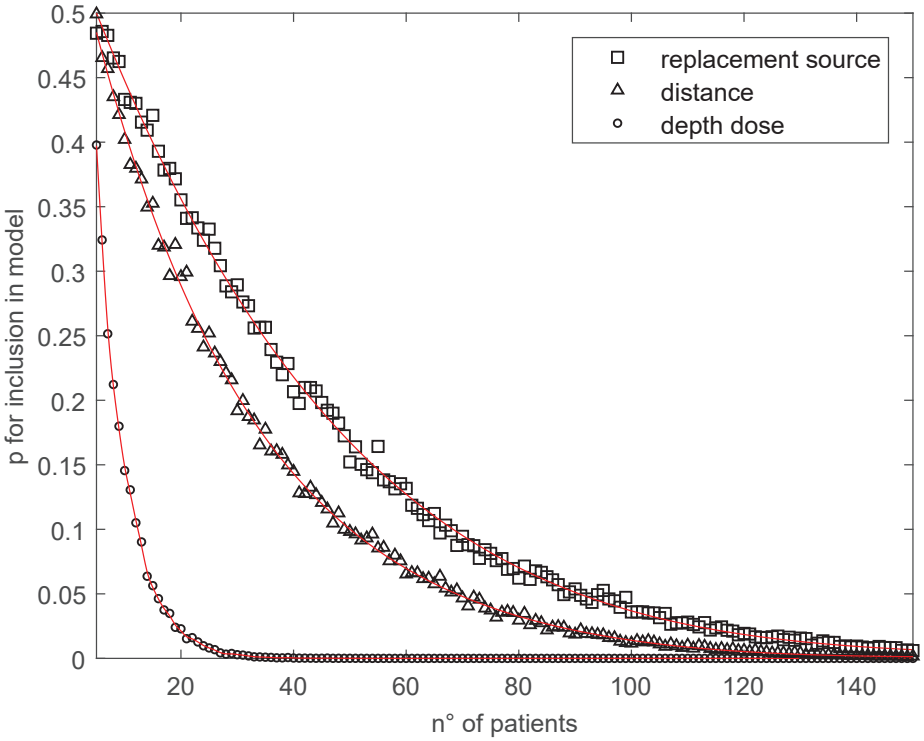

mp_13379_f3.eps